Computer-Aided Design of Microstrip Filters by Iterated Analysis

GARY T. ROAN AND KAWTHAR A. ZAKI, SENIOR MEMBER, IEEE

Abstract —An iterative method for the design of microstrip low-pass elliptic function filters is described. The method, which is a direct extension of [1], determines the microstrip line parameters that produce the same locations of the frequencies of transmission zeros and reflection zeros of an equivalent lumped-element prototype. Effects of the discontinuities at the junctions are easily accounted for in the iteration. A design example is included, and an experimental seventh-order filter designed and constructed using the procedure gives measured results which agree closely with theory.

I. Introduction

THIS PAPER is an extension to the distributed element case of a technique originally introduced in [1] for the design of lumped-element low-pass filters.

Low-pass filters implemented on microstrip offer an attractive alternative to other media for miniaturization, low manufacturing costs, and its potential for integration with other MIC or MMIC components. Techniques for realization of such filters on thin, moderate-to-high relative dielectric constant substrates (e.g., alumina), with cut-off frequencies in the C band and higher, often lead to unsatisfactory results (e.g., inclusion of redundant transmission line elements [2]–[4], impractical impedance levels, long line lengths, etc.). Similar problems also rise when semilumped element techniques for Chebyshev filter realizations are used [5].

In [6], a good method for the synthesis and realization of microstrip low-pass filters was presented. This method uses the complete equivalent circuit of a rectangular microstrip as the building block to synthesize the desired filter response, and thereby avoids the use of redundant elements. To use this technique, it is essential first to perform the synthesis of a lumped-element prototype filter (or find the element values from tables) using the well-known conventional insertion-loss theory [7].

In this paper an alternative approach is presented for the design of microstrip low-pass filters of higher order. The approach extends the principles developed in [1] (which deals with the lumped-element case) to the distributed parameter case. The essence of this method is to iteratively adjust a set of the filter's element values until the zeros, poles, and the scale factor of the characteristic function of the microstrip filter match their desired values. The method requires only simple analysis, avoids complications normally associated with network synthesis of high-degree networks, and easily takes into account the effects of all discontinuities and parasitics. The synthesis may not be optimum, since the transmission and reflection zeros are optimized for the lumped-element case. In practice, this results in a nonequiripple passband with lower ripple near the band edges.

In Section II the design procedure is described. The process of solution of the poles and zeros of the filter's characteristic function is outlined. The method of analysis uses the simple chain matrix multiplication of the cascaded elements. This allows the effects of the discontinuities to be included as "fixed" elements in the cascade. Since the iterative process requires the calculation of partial derivatives of the response with respect to the parameters of the elements, an efficient method for doing this is presented.

Section III presents results of the application of the method. Convergence and accuracy of the iteration process is examined. Considerations for practical implementation of filters and numerical results of typical designs illustrating these considerations are presented.

Section IV presents measured results on a seventh-order experimental filter and compares the measurements with theory. Conclusions and discussions are included in Section V.

II. Design Procedure

The design procedure starts by finding the characteristic function $\hat{K}(s)$ of a low-pass prototype which meets the loss specifications with an equal-ripple passband. This can be done by using one of several standard approximation procedures [8]. The result of this step yields the filter order n, the passband ripple α_p, the transmission zeros ω_{∞_k}, and the reflection zeros ω_{0_k} of a lumped-element prototype, shown in Fig. 1. The characteristic function is given by

$$\hat{K}(s) = \epsilon \frac{f(s)}{p(s)} \tag{1a}$$

Manuscript received November 3, 1987; revised June 4, 1988.

G. T. Roan is with the Naval Research Laboratory, Tactical Electronic Warfare Division, Washington, DC 20375.

K. A. Zaki is with the Department of Electrical Engineering, University of Maryland, College Park, MD 20742.

IEEE Log Number 8823699.

0018-9480/88/1100-1482$01.00

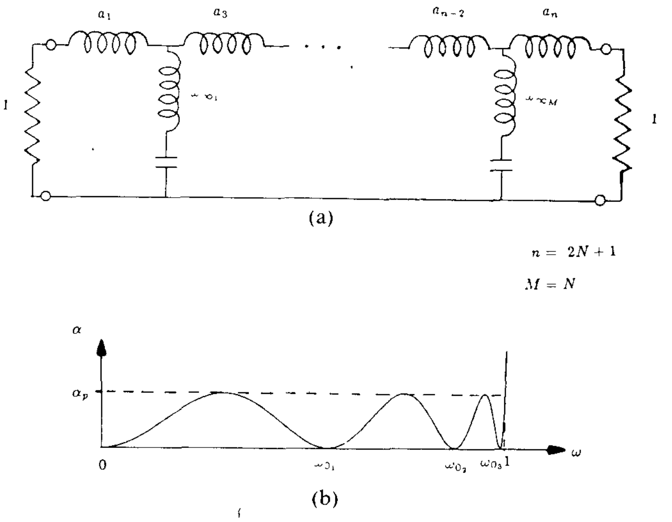

Fig. 1. Symmetric low-pass filter prototype (a) and its passband response (b) shown for the case $n=7$ ($N=3$).

where

$$f(s)=s\prod_{k=1}^{N}\left(s^2+\omega_{0_k}^2\right) \tag{1b}$$

$$p(s)=\prod_{i=1}^{M}\left(s^2+\omega_{\infty_i}^2\right) \tag{1c}$$

and

$$\epsilon=10^{0.1\alpha_p}-1 \tag{1d}$$

$$M\leqslant N,\qquad 1>\omega_{0_k},\ \omega_{\infty_i}>1.$$

The filter insertion loss ratio, defined as the ratio of the maximum available source power to the output power in the termination, is related to $\hat{K}(s)$ by

$$H(s)H(-s)=1+\hat{K}(s)\hat{K}(-s). \tag{2}$$

In the following discussion it will be assumed that the filter order n is odd ($n=2N+1$) and that it possesses the maximum number of finite transmission zeros (i.e., $M=N$). Under these assumptions the circuit will be symmetric (i.e., the two port parameters $Z_{11}=Z_{22}$). From a practical viewpoint this assumption does not represent any significant restrictions. However, for n even, or for $M<N$, the modifications to the design procedure are straightforward. A microstrip circuit which approximates the behavior of the lumped-element prototype is shown in Fig. 2. This circuit consists of a cascade of short lengths of high-impedance lines of a characteristic impedance Z_{0_h}, alternating with shunt open-circuit stubs. The lengths of the shunt stubs are chosen such that they produce the loss poles ω_{∞_k} (i.e., the poles of $\hat{K}(s)$).

Equivalent circuits of the two types of discontinuities encountered in the filter of Fig. 2 are shown in Fig. 3. For the T junction of a stub with the high-impedance line [9] (Fig. 3(a)), at terminal plane T_1, the open-circuit stub's equivalent circuit, including the end's fringing capacitance C_{f_k}, is shown in Fig. 3(b). The stub lengths d_k are chosen to be

$$d_k=\frac{v_k}{\omega_{\infty_k}}\tan^{-1}\left[\frac{1-\omega_{\infty_k}^2L_kC_{f_k}}{\omega_{\infty_k}C_{f_k}Z_{0_k}+\left(\omega_{\infty_k}L_k/Z_{0_k}\right)}\right]\qquad k=1,2,\cdots,M$$

$$\approx\frac{v_k}{\omega_{\infty_k}}\left[\frac{\pi}{2}-\frac{\omega_{\infty_k}C_{f_k}Z_{0_k}+\left(\omega_{\infty_k}L_k/Z_{0_k}\right)}{1-\omega_{\infty_k}^2L_kC_{f_k}}\right] \tag{3}$$

where v_k = propagation velocity on the stub, Z_{0_k} = stub's characteristic impedance, and L_k = the stub's series discontinuity inductance of the T junction. The above choices of the shunt stub lengths ensure that the characteristic function $K(s)$ of the network will have the correct poles (i.e., poles of $\hat{K}(s)$). The next step in the design procedure is to iteratively change the line lengths l_i, $i=1,3,5,\cdots,n$ and stub characteristic impedances Z_{0_k}, $k=1,2,\cdots,M$ such as to force the characteristic function $K(s)$ to have the same zeros as $\hat{K}(s)$ and the multiplying constant ϵ. A systematic way to accomplish this is described below [1].

The chain matrix of the filter, which is a lossless reciprocal 2-port, at any given frequency ω can be written as

$$\begin{bmatrix}V_1\\ I_1\end{bmatrix}=\begin{bmatrix}A & jB\\ jC & D\end{bmatrix}\begin{bmatrix}V_2\\ -I_2\end{bmatrix} \tag{4}$$

where A, B, C, and D are all real functions of ω. The input reflection coefficient ρ of the filter terminated in the normalized unit load is easily shown to be given by

$$\rho=\frac{(A-D)+j(B-C)}{(A+D)+j(B+C)}. \tag{5}$$

The insertion voltage ratio $H(j\omega)$ and the characteristic function $K(j\omega)$ are given respectively by [1]

$$2H(j\omega)=(A+D)+j(B+C) \tag{6}$$

$$2K(j\omega)=(A-D)+j(B-C). \tag{7}$$

If the chain matrix of the filter is evaluated at the zeros of $\hat{K}(s)$, all of which are simple and lie on the $j\omega$ axis, then at each of these zeros (7) gives two real equations:

$$A-D=0\quad\text{and}\quad B-C=0. \tag{8}$$

Equation (8), when applied at each of the given N reflection zeros of the filter, result in $2N$ nonlinear equations in the $n(=2N+1)$ unknown element values. These unknowns (see Fig. 2) are the line lengths $l_1, l_3,\cdots,l_n$ and the shunt stub normalized characteristic impedances $Z_{0_1}, Z_{0_2},\cdots,Z_{0_M}$. An additional equation is obtained by matching the behavior of $K(s)$ and $\hat{K}(s)$ around $s=0$ in an analogous way to the lumped-element case [1]. The result of this process (ignoring contributions from discontinuities) gives

$$2k\sum_{i=1}^{n}m_i=\frac{\left(Z_{0_h}-1/Z_{0_h}\right)}{v_h}\sum_{i=1}^{N}l_{2i+1}-\sum_{k=1}^{M}\frac{1}{Z_{0_k}}\frac{d_k}{v_k} \tag{9}$$

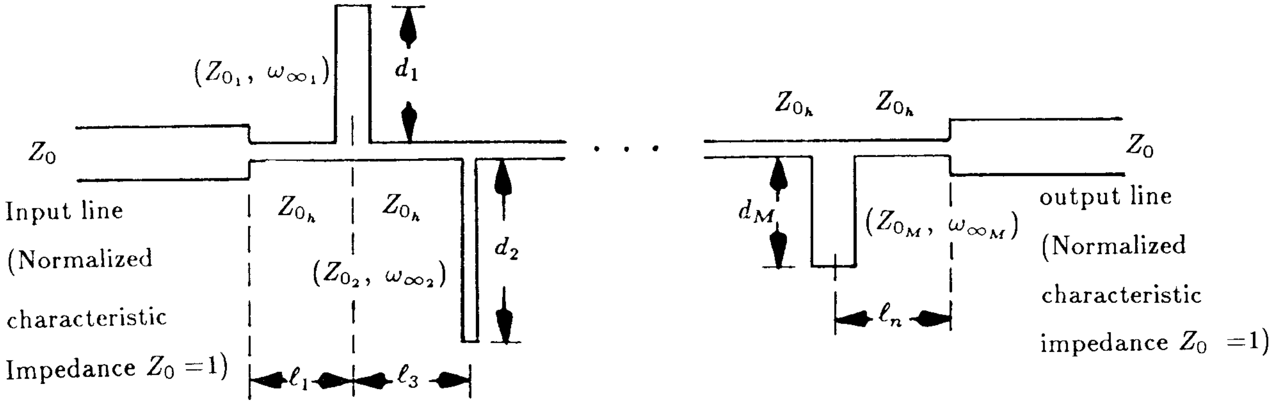

Fig. 2. Microstrip realization of the filter of Fig. 1.

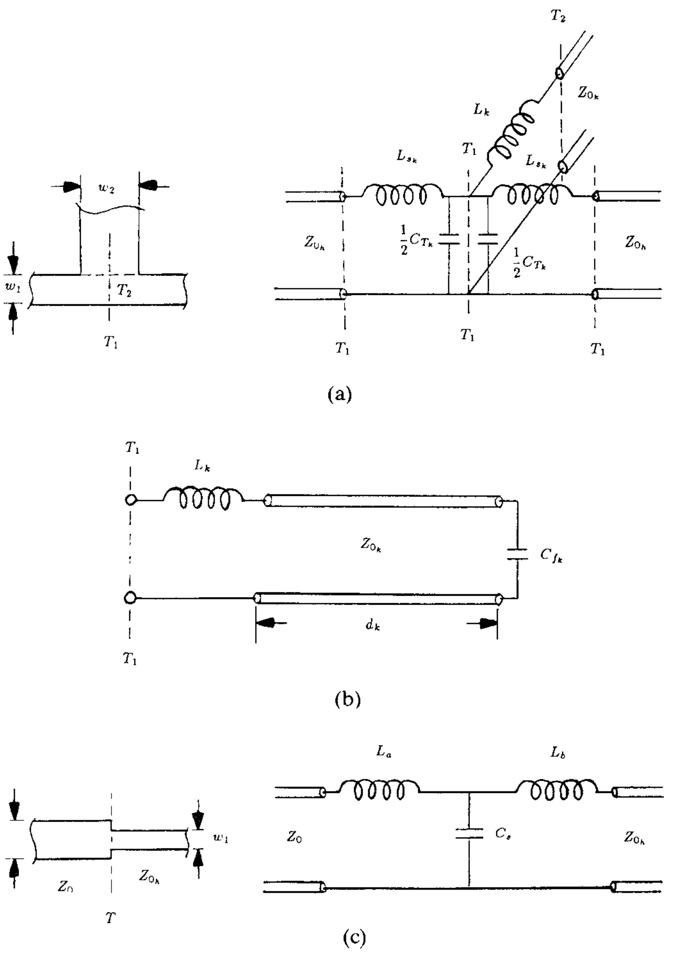

Fig. 3. (a) Equivalent circuit of the T-junction discontinuity. (b) Equivalent circuit of the open stub at terminal plane T_1, including fringing capacitance C_f. (c) Equivalent circuit at junction between input and output lines and the first filter section.

where

$$m_i = \sqrt{\frac{\omega_{\infty_i}^2 - 1}{\omega_{\infty_i}^2}} \tag{10a}$$

$$k^2 = 10^{\alpha_p/10} - 1 \tag{10b}$$

and where α_p is the passband ripple of the low-pass prototype. (Note that all impedances Z_{0_h}, Z_{0_k} are normalized to the input and output line impedances Z_0.) Proof of (9) follows the same steps as the lumped case in [1].

Solution of the n equations (8) and (9) is most conveniently accomplished iteratively using Newton's method, for which the derivatives of the equations with respect to the variables are needed. Derivatives of the chain matrix are efficiently computed as indicated below [1], [10].

The overall chain matrix T of the filter is the product of the chain matrices of the individual cascaded sections [10]

$$T(\boldsymbol{x}) = T_1 T_2 \cdots T_{j-1} T_j T_{j+1} \cdots T_n \tag{11}$$

where T_i is the chain matrix of the ith section, $i = 1, 2, \cdots, n$, $\boldsymbol{x}$ is the vector of variable network parameters (i.e., line lengths $l_1, l_3, \cdots, l_n$ and characteristic impedances $Z_{0_1}, Z_{0_2}, \cdots, Z_{0_M}$). If x_i belongs to section j, then the partial derivative of $T(\boldsymbol{x})$ with respect to x_i is given by [10]

$$\frac{\partial T(\boldsymbol{x})}{\partial x_i} = T_1 T_2 \cdots T_{j-1} \frac{\partial T_j}{\partial x_i} T_{j+1} \cdots T_n. \tag{12}$$

Explicit expressions for the individual chain matrices T_j and their derivatives $\partial T_j / \partial x_i$, including the discontinuity effects, are summarized in Fig. 4.

Let the values of the left-hand sides of (8) and (9), as computed from the approximate network, be assembled in any order into a vector $\boldsymbol{g}$, and let the values of the right-hand side of these equations be assembled, in the same order, into a vector $\hat{\boldsymbol{g}}$. Let the vector $\boldsymbol{x}$ of the element values have the components defined in Fig. 4 ($x_{2k-1} = l_{2k-1}$, $k = 1, \cdots, M+1$, $x_{2_k} = Z_{0_k}$, $k = 1, 2, \cdots, M$), and let the partial derivatives of the left-hand side of (8) and (9) with respect to x_i form the Jacobian matrix $\underline{J}$. The Newton method then gives the correction $\Delta \boldsymbol{x}$ to an approximate vector $\boldsymbol{x}$ as the solution of the n linear equations [1]:

$$\underline{J} \Delta \boldsymbol{x} = \hat{\boldsymbol{g}} - \boldsymbol{g}. \tag{13}$$

$\underline{J}$ and $\boldsymbol{g}$ are formed simultaneously, two rows at a time, from the two analyses at each frequency of zero loss as obtained from Fig. 4. Entries for $\underline{J}$ corresponding to (9) are simply obtained as $(Z_{0_h} - 1/Z_{0_h})/v_h$ for $x_{2k+1} = l_{2k+1}$ or d_k / v_k for $x_{2k} = Z_{0_k}$.

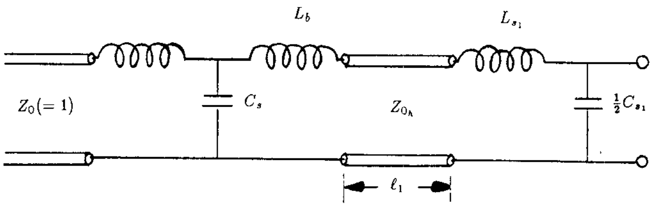

$$x_1 = \ell_1, \quad \theta_1 = \frac{\omega \ell_1}{v_h}$$

$$T_1 = T_A \begin{bmatrix} \cos\theta_1 & j\frac{Z_{0_h}}{Z_0}\sin\theta_1 \\ j\frac{Z_0}{Z_{0_h}}\sin\theta_1 & \cos\theta_1 \end{bmatrix} T_B$$

$$T_A = \begin{bmatrix} 1 & j\frac{\omega L_a}{Z_0} \\ 0 & 1 \end{bmatrix} \begin{bmatrix} 1 & 0 \\ jZ_0\omega C_s & 1 \end{bmatrix} \begin{bmatrix} 1 & j\frac{\omega L_b}{Z_0} \\ 0 & 1 \end{bmatrix}$$

$$T_B = \begin{bmatrix} 1 & j\frac{\omega L_{s_1}}{Z_0} \\ 0 & 1 \end{bmatrix} \begin{bmatrix} 1 & 0 \\ \frac{1}{2}jZ_0\omega C_{s_1} & 1 \end{bmatrix}$$

$$\frac{\partial T_1}{\partial x_1} = \frac{\omega}{v_h} T_A \begin{bmatrix} -\sin\theta_1 & j\frac{Z_{0_h}}{Z_0}\cos\theta_1 \\ j\frac{Z_0}{Z_{0_h}}\sin\theta_1 & -\sin\theta_1 \end{bmatrix} T_B$$

(a)

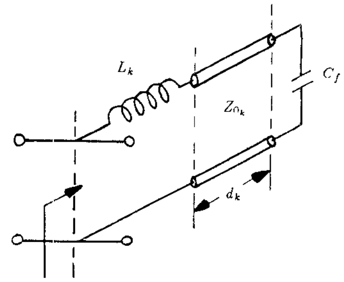

For $k = 1, 2, \cdots, M$

$$x_{2k} = Z_{0_k}, \quad \phi_k = \frac{\omega d_k}{v_k}$$

$$-\frac{1}{B_k} = \frac{\omega L_k}{Z_0} + \frac{Z_{0_k}}{Z_0}\left[\frac{\omega C_f Z_{0_k}\tan\phi_k - 1}{\omega C_f Z_{0_k} + \tan\phi_k}\right] \quad jB_l$$

$$T_{2k} = \begin{bmatrix} 1 & 0 \\ jB_k & 1 \end{bmatrix}, \quad \frac{\partial T_{2k}}{\partial x_{2k}} = \begin{bmatrix} 0 & 0 \\ j\frac{\partial B_k}{\partial x_{2k}} & 0 \end{bmatrix}$$

$$\frac{\partial B_k}{\partial x_{2k}} = B_k^2 Z_0^2\left[\left(1 + \frac{\omega L_k}{Z_{0_k}} + \frac{1}{Z_{0_k}B_k}\right)\frac{\omega C_{fk} Z_{0_k}\tan\theta_k}{\omega C_{fk} Z_{0_k} - \tan\theta_k} - \left(\frac{\omega L_k}{Z_{0_k}} - \frac{1}{Z_{0_k}B_k}\right)\right]$$

(b)

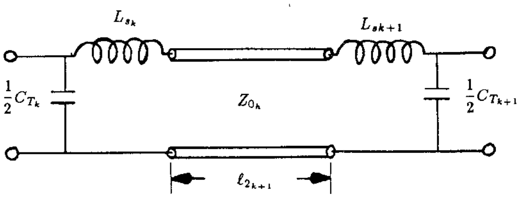

$$x_{2k+1} = \ell_{2k+1} \quad k = 1, 2, \cdots, M-1$$

$$\theta_{2k+1} = \frac{\omega \ell_{2k+1}}{v_h}$$

$$T_{2k+1} = T_A \begin{bmatrix} \cos\theta_{2k+1} & j\frac{Z_{0_h}}{Z_0}\sin\theta_{2k+1} \\ j\frac{Z_0}{Z_{0_h}}\sin\theta_{2k+1} & \cos\theta_{2k+1} \end{bmatrix} T_B$$

$$T_A = \begin{bmatrix} 1 & 0 \\ jZ_0\omega C_{T_k} & 1 \end{bmatrix} \begin{bmatrix} 1 & j\omega\frac{L_{sk}}{Z_0} \\ 0 & 1 \end{bmatrix}, \quad T_B = \begin{bmatrix} 1 & j\frac{\omega L_{sk+1}}{Z_0} \\ 0 & 1 \end{bmatrix} \begin{bmatrix} 1 & 0 \\ jZ_0\omega C_{Tk+1} & 1 \end{bmatrix}$$

$$\frac{\partial T_{2k+1}}{\partial x_{2k+1}} = \frac{\omega}{v_h} T_A \begin{bmatrix} -\sin\theta_{2k+1} & j\frac{Z_{0_h}}{Z_0}\cos\theta_{2k+1} \\ \frac{jZ_0}{Z_{0_h}}\cos\theta_{2k+1} & -\sin\theta_{2k+1} \end{bmatrix} T_B$$

(c)

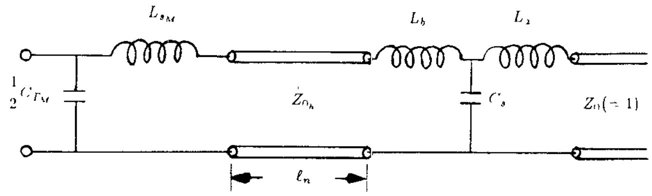

$$x_n = \ell_n \quad n = 2M-1 \quad \theta_n = \frac{\omega \ell_n}{v_h}$$

$$T_n = T_A \begin{bmatrix} \cos\theta_n & j\frac{Z_{0_h}}{Z_0}\sin\theta_n \\ j\frac{Z_0}{Z_{0_h}}\sin\theta_n & \cos_n \end{bmatrix} T_B$$

$$T_A = \begin{bmatrix} 1 & 0 \\ \frac{1}{2}Z_0\omega C_{T_M} & 1 \end{bmatrix} \begin{bmatrix} 1 & j\frac{\omega L_{sM}}{Z_0} \\ 0 & 1 \end{bmatrix}, \quad T_B = \begin{bmatrix} 1 & j\frac{\omega L_b}{Z_0} \\ 0 & 1 \end{bmatrix} \begin{bmatrix} 1 & 0 \\ jZ_0\omega C_s & 1 \end{bmatrix} \begin{bmatrix} 1 & j\frac{\omega L_a}{Z_0} \\ 0 & 1 \end{bmatrix}$$

$$\frac{\partial T_n}{\partial x_n} = \frac{\omega}{v_h} T_A \begin{bmatrix} -\sin\theta_n & j\frac{Z_{0_h}}{Z_0}\cos\theta_n \\ j\frac{Z_{0_h}}{Z_0}\cos\theta_n & -\sin\theta_n \end{bmatrix} T_B$$

(d)

Fig. 4. (a) Equivalent circuit, chain matrix, and its derivative of input section, including discontinuities. (b) Equivalent circuit, chain matrix, and its derivative for shunt stub, including discontinuities. (c) Equivalent circuit, chain matrix, and its derivative for a typical high-impedance line section, including discontinuities. (d) Equivalent circuit, chain matrix, and its derivative for the output section, including discontinuities.

III. Numerical Results

A computer program was implemented to carry out the design procedure described in the previous section. The line lengths l_{2k+1}, and stub characteristic impedances Z_{0_k}, $k = 1, 2, \cdots, M$ are initially chosen to be $\lambda/16$ and Z_0, respectively. The value Z_{0_h} of the high-impedance lines is chosen to provide the highest possible value for a reasonable line width on the substrate material ($2Z_0 \leqslant Z_{0_h} \leqslant 2.5Z_0$). Then the discontinuities of the equivalent circuits of Fig. 3 are determined from these line dimensions according to the formulas given in [9]. The stub lengths d_k, $k = 1, 2, \cdots, M$ are then determined from (3). Then the iterative procedure is started. In each step of the iteration, after the new shunt stub impedances are obtained, the corresponding line widths are determined and the new corresponding discontinuity reactances computed, which are then used in the next step of the iteration. This procedure has been tried for several cases and was found to always converge in a number of iterations which is dependent on the filter's order n. For $n \leqslant 7$ only about ten iterations are needed, while for $n \geqslant 12$ typically 20 to 25 iterations are required.

An example of a seven-section low-pass filter is presented below. The filter has a cutoff frequency of 4 GHz, a minimum stopband attenuation of 40 dB, and a passband ripple of 0.1733 dB (i.e., maximum passband VSWR = 1.5). Table I gives the locations of the normalized passband zero reflection points and stopband attenuation poles. The final normalized adjusted values of the line lengths and shunt stub impedances for this filter are given in Table II.

The calculated responses of the lumped-element prototype filter and the distributed parameter filter are shown in

TABLE I
NORMALIZED REFLECTION ZEROS AND TRANSMISSION ZEROS OF A SEVEN-ELEMENT FILTER

Number of elements	7
Pass band ripple (dB)	.1773
Minimum stop band attenuation (dB)	40
Normalized reflection zeros ω_{0_1}	0.5355906
ω_{0_2}	0.8586568
ω_{0_3}	0.9860456
Normalized transmission zeros ω_{∞_1}	1.230000
ω_{∞_2}	1.500000
ω_{∞_3}	1.880000

TABLE II
NORMALIZED CHARACTERISTIC IMPEDANCES, LINE, AND STUB LENGTHS OF A SEVEN-ELEMENT FILTER

Element	Normalized Impedance	Line length (wave lengths)
ℓ_1	2.0000	0.095777
d_1	1.1171	0.14143
ℓ_3	2.0000	0.15047
d_2	2.0345	0.20779
ℓ_5	2.0000	0.13935
d_3	1.5109	0.17229
ℓ_7	2.0000	0.081761

Fig. 5. The passband insertion loss response (Fig. 5(a)) of the distributed parameter filter does not exhibit the equal ripple behavior, but shows a decreasing ripple level closer to the band edge. The stopband of Fig. 5(b) shows the spurious response of the distributed parameter filter starting at approximately twice its cutoff frequency.

IV. EXPERIMENTAL RESULTS

To verify the design procedure, a seven-element low-pass elliptic function filter with a 0.17 dB passband ripple, 40 dB minimum cutoff band attenuation, and 4 GHz cutoff frequency was designed, constructed, and tested. The filter was realized on an alumina substrate 0.025 inches thick. The enlarged conductor pattern of this filter is shown in Fig. 6. This filter is constructed according to an earlier version of the design procedure described in Section II. In that earlier version the transmission zeros were realized as shunt connected semilumped stubs as described in Section II. Each semilumped $L-C$ circuit is realized as shown in Fig. 6 by a short length of high-impedance line (approximating L) in cascade with a short length of low-impedance line (approximating C). It was later recognized that single shunt stubs are simpler to use in terms of the design procedure and practical realization. The filter responses using either method were almost identical. The measured and computed insertion and return loss variations with frequency of the filter (modeled precisely using the conductor pattern of Fig. 6) are shown in Fig. 7. The wide-band measured and computed insertion loss responses are shown in Fig. 8, showing the spurious responses up to 12 GHz. Agreement between the measurements and calculations are quite good, in both the passband, the stopband, as well as the far-out spurious responses. The transmission zeros of the insertion loss are quite close to their predicted values, and the minimum out of band response of 38 dB is also in close agreement with

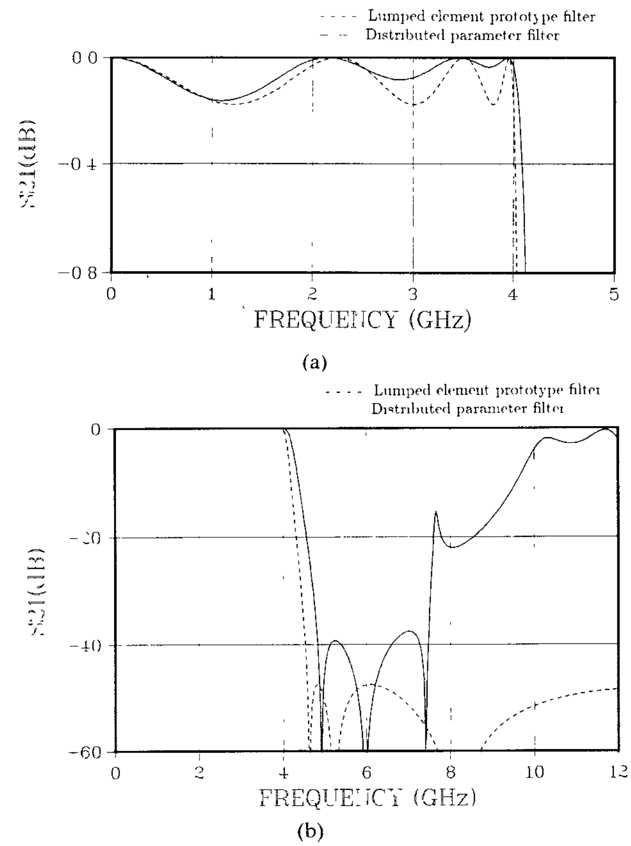

Fig. 5. (a) Calculated passband insertion loss responses. (b) Calculated wideband insertion loss responses.

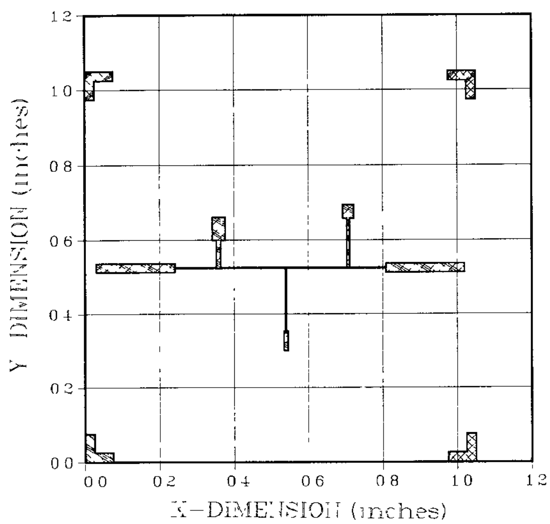

Fig. 6. Microstrip distributed filter.

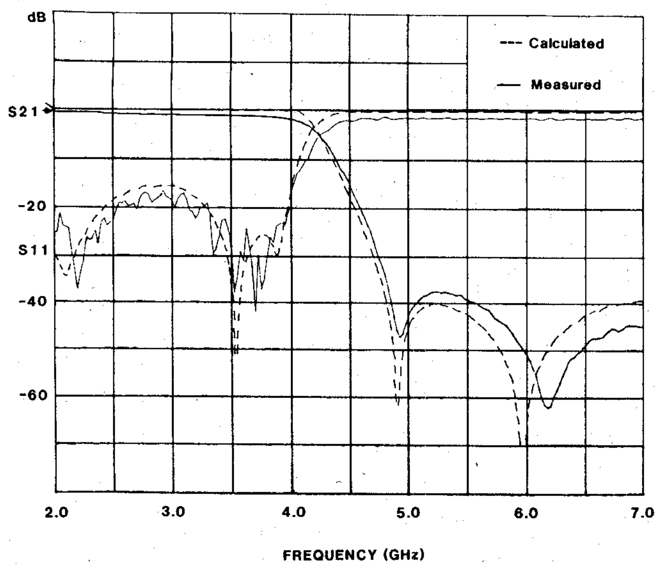

Fig. 7. Calculated and measured response of the filter.

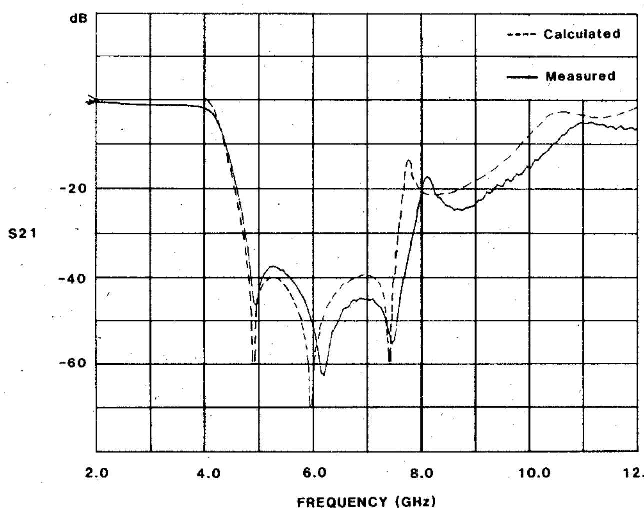

Fig. 8. Measured and computed wideband insertion loss response of the filter showing its far-out spurious responses.

the 40 dB design value. The return loss is also quite close to the theory. This filter fits on a substrate which measures 1.0×1.0 inches and its width could be reduced to 0.5 inches, as seen from Fig. 6.

V. Conclusions

The design process described in this paper proves to be an extremely well-conditioned approach which gives accurate results even for filters of high order. The procedure combines simplicity and efficiency and easily accounts for the effects of all the discontinuities in the circuit. Measured results obtained from the experimental filter constructed to verify the procedure showed good agreement with theory. The filter is compact and can be easily integrated with MIC subsystems.

References

[1] H. J. Orchard, "Filter design by iterated analysis," *IEEE Trans. Circuits Systs.*, vol. CAS-32, pp. 1089–1096, Nov. 1985.

[2] B. M. Schiffman and L. Young, "Design tables for an elliptic function band-stop filter ($N = 5$)," *IEEE Trans. Microwave Theory Tech.*, vol. MTT-34, pp. 474–482, Oct. 1986.

[3] R. Levy and I. Whiteley, "Synthesis of distributed elliptic function filters from lumped-constant prototypes," *IEEE Trans. Microwave Theory Tech.*, vol. MTT-14, pp. 506–517, Nov. 1966.

[4] J. A. G. Malherbe, "TEM pseudoelliptic-function bandstop filters using non-commensurate lines," *IEEE Trans. Microwave Theory Tech.*, vol. MTT-24, pp. 242–248, May 1976.

[5] G. L. Matthaei, L. Young, and E. M. T. Jones, *Microwave Filter Impedance Matching Networks and Coupling Structures*. New York: McGraw–Hill Book Company, 1964.

[6] F. Giannini, M. Salerno, and R. Sorrentino, "Design of low-pass elliptic filter by means of cascaded microstrip rectangular elements," *IEEE Trans. Microwave Theory Tech.*, vol. MTT-30, pp. 1348–1353, Sept. 1982.

[7] S. Darlington, "Synthesis of reactance 4-poles which produce prescribed insertion loss characteristics," *J. Math. Phys.*, vol. 18, pp. 257–353, Sept. 1939.

[8] G. C. Temes and S. K. Mitra, *Modern Filter Theory and Design*. New York: Wiley, 1973.

[9] K. C. Gupta, R. Gorg, and Rakesh Chadha, *Computer-Aided Design of Microwave Circuits*. Dedham, MA: Artech House, Inc., 1981, pp. 189–197.

[10] K. W. Iobst and K. A. Zaki, "An optimization technique for lumped-distributed two ports," *IEEE Trans. Microwave Theory Tech.*, vol. MTT-30, pp. 2167–2171, Dec. 1982.

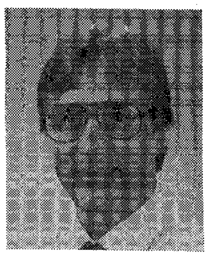

Gary T. Roan received the B.S. degree in physics from the Pennsylvania State University, University Park, in 1977, and the M.S. degree in electrical engineering from the University of Maryland, College Park, in 1987. He is currently working towards a Ph.D. degree in electrical engineering at the University of Maryland.

Since 1979 he has been employed by the Tactical Electronic Warfare Division of the Naval Research Laboratory in Washington, D.C., where he is involved with research and development of offboard electronic countermeasures systems. His research interests are in the area of computer-aided design of microwave and solid state devices.

Kawthar A. Zaki (SM'85) received the B.S. degree with honors from Ain Shams University, Cairo, Egypt, in 1962, and the M.S. and Ph.D. degrees from the University of California, Berkeley, in 1966 and 1969, respectively, all in electrical engineering.

From 1962 to 1964 she was a Lecturer in the Department of Electrical Engineering, Ain Shams University. From 1965 to 1969 she held the position of Research Assistant in the Electronic Research Laboratory, University of California, Berkeley. She joined the Electrical Engineering Department, University of Maryland, College Park, in 1970, where she is presently a Professor. Her research interests are in the areas of electromagnetics, microwave circuits, optimization, and computer-aided design.

Dr. Zaki is a member of Tau Beta Pi.